NASA/TM—2005-213442

Unitized Regenerative Fuel Cell System Gas Storage-Radiator Development

Kenneth A. Burke
Glenn Research Center, Cleveland, Ohio

Ian Jakupca
Analex Corporation, Cleveland, Ohio

October 2005

The NASA STI Program Office . . . in Profile

Since its founding, NASA has been dedicated to the advancement of aeronautics and space science. The NASA Scientific and Technical Information (STI) Program Office plays a key part in helping NASA maintain this important role.

The NASA STI Program Office is operated by Langley Research Center, the Lead Center for NASA's scientific and technical information. The NASA STI Program Office provides access to the NASA STI Database, the largest collection of aeronautical and space science STI in the world. The Program Office is also NASA's institutional mechanism for disseminating the results of its research and development activities. These results are published by NASA in the NASA STI Report Series, which includes the following report types:

- TECHNICAL PUBLICATION. Reports of completed research or a major significant phase of research that present the results of NASA programs and include extensive data or theoretical analysis. Includes compilations of significant scientific and technical data and information deemed to be of continuing reference value. NASA's counterpart of peer-reviewed formal professional papers but has less stringent limitations on manuscript length and extent of graphic presentations.

- TECHNICAL MEMORANDUM. Scientific and technical findings that are preliminary or of specialized interest, e.g., quick release reports, working papers, and bibliographies that contain minimal annotation. Does not contain extensive analysis.

- CONTRACTOR REPORT. Scientific and technical findings by NASA-sponsored contractors and grantees.

- CONFERENCE PUBLICATION. Collected papers from scientific and technical conferences, symposia, seminars, or other meetings sponsored or cosponsored by NASA.

- SPECIAL PUBLICATION. Scientific, technical, or historical information from NASA programs, projects, and missions, often concerned with subjects having substantial public interest.

- TECHNICAL TRANSLATION. English-language translations of foreign scientific and technical material pertinent to NASA's mission.

Specialized services that complement the STI Program Office's diverse offerings include creating custom thesauri, building customized databases, organizing and publishing research results . . . even providing videos.

For more information about the NASA STI Program Office, see the following:

- Access the NASA STI Program Home Page at ***http://www.sti.nasa.gov***

- E-mail your question via the Internet to help@sti.nasa.gov

- Fax your question to the NASA Access Help Desk at 301–621–0134

- Telephone the NASA Access Help Desk at 301–621–0390

- Write to:
  NASA Access Help Desk
  NASA Center for AeroSpace Information
  7121 Standard Drive
  Hanover, MD 21076

NASA/TM—2005-213442

Unitized Regenerative Fuel Cell System Gas Storage-Radiator Development

Kenneth A. Burke
Glenn Research Center, Cleveland, Ohio

Ian Jakupca
Analex Corporation, Cleveland, Ohio

Prepared for the
Power Systems Conference
sponsored by the Society of Automotive Engineers
Reno, Nevada, November 2–4, 2004

National Aeronautics and
Space Administration

Glenn Research Center

October 2005

Available from

NASA Center for Aerospace Information
7121 Standard Drive
Hanover, MD 21076

National Technical Information Service
5285 Port Royal Road
Springfield, VA 22100

Available electronically at http://gltrs.grc.nasa.gov

Unitized Regenerative Fuel Cell System Gas Storage-Radiator Development

Kenneth A. Burke
National Aeronautics and Space Administration
Glenn Research Center
Cleveland, Ohio 44135

Ian Jakupca
Analex Corporation
Cleveland, Ohio 44135

Summary

High-energy-density regenerative fuel cell systems that are used for energy storage require novel approaches to integrating components in order to preserve mass and volume. A lightweight unitized regenerative fuel cell (URFC) energy storage system concept is being developed at the NASA Glenn Research Center. This URFC system minimizes mass by using the surface area of the hydrogen and oxygen storage tanks as radiating heat surfaces for overall thermal control of the system. The waste heat generated by the URFC stack during charging and discharging is transferred from the cell stack to the surface of each tank by loop heat pipes, which are coiled around each tank and covered with a thin layer of thermally conductive carbon composite. The thin layer of carbon composite acts as a fin structure that spreads the heat away from the heat pipe and across the entire tank surface.

Two different-sized commercial-grade composite tanks were constructed with integral heat pipes and tested in a thermal vacuum chamber to examine the feasibility of using the storage tanks as system radiators. The storage tank-radiators were subjected to different steady-state heat loads and varying heat load profiles. The surface emissivity and specific heat capacity of each tank were calculated. In the future, the results will be incorporated into a model that simulates the performance of similar radiators using lightweight, space-rated carbon composite tanks.

Introduction

The NASA Glenn Research Center Energetics Research Program is funding the development of a unitized regenerative fuel cell system (URFCS) that will use a URFC as the main component of a lightweight, compact energy storage system. The goal of this program is to demonstrate the feasibility of a URFC energy storage system that can achieve an energy density of >400 Wh per kilogram of mass. While the program does not have the funding to produce actual flight-weight hardware, enough development and testing will be completed such that the >400 Wh per kilogram goal can be confidently projected. To achieve this goal, an innovative system concept was conceived and was described in an earlier report (ref. 1).

Ancillary components supporting this system concept, as well as supporting other fuel cell and electrolysis systems, are currently being developed.

One of the aspects of the design concept being developed is the use of a loop heat pipe system to control the temperature of the URFC stack and to transfer the waste heat to the surface of the two gas storage tanks where it is radiated to space. The gas storage tanks, being the two components with the greatest external surface area, act as the URFCS radiator as well as the storage containers for the gaseous reactants. This approach saves the mass of adding a separate heat exchanger or radiator. To the best knowledge of the authors, this is the first attempt to incorporate heat pipes into pressure vessels or into a

fuel cell system of any kind. The methods of heat pipe incorporation as well as the materials of construction are useful for applications other than URFC energy storage.

To aid the reader, a listing of acronyms and symbols used in this report is given in the appendix.

Background

As an energy storage system, an RFCS "charges" and "discharges" like a rechargeable battery. A more detailed comparison of the RFCS to batteries has been described in an earlier report (ref. 2). While charging, the RFCS operates the electrolysis process, which splits water into hydrogen and oxygen. While discharging, the RFCS operates the fuel cell process, which combines hydrogen and oxygen and produces electricity.

An RFCS combines two energy conversion devices, an electrolyzer and a fuel cell, to form the core of an energy storage system. Because of water stoichiometry, an RFCS generally uses twice the hydrogen gas storage volume as it does oxygen. The fuel cell and electrolyzer require that the waste heat be removed to maintain proper performance.

The key advantage of the URFCS over the RFCS is that the URFCS has a single cell stack that does both the process of water electrolysis as well as the process of recombination of the hydrogen and oxygen gas to produce electricity. Since only one cell stack is needed instead of one electrolysis cell stack and one fuel cell stack, a substantial amount of mass is saved because the cell stacks are major mass components of an RFCS. Depending on the operating current density of the electrochemical cell stacks, the mass associated with either the water electrolysis cell stack or the fuel cell stack is typically 500 to 1000 W per kilogram (2.2 lb) of stack mass (ref. 2). Therefore, as an example, for a 10 kW RFCS, the electrolysis cell stack and fuel cell stack would each have approximately a 10 to 20 kg (22.1 to 44.1 lb) mass (a total of 20 to 40 kg or 44.1 to 88.2 lb), whereas the URFCS would have only a single 10- to 20-kg (22.1- to 44.1-lb) cell stack. Besides saving the mass of one cell stack, the plumbing, wiring, structural mounting, and ancillary equipment for one cell stack are also eliminated.

Figure 1 shows a schematic of a URFCS concept being developed at NASA Glenn. The system consists of the URFC stack, a gas storage system, pressure controls between the URFC stack and the gas storage system, a water storage tank, a heat pipe thermal control system, and a power system control interface.

As the URFCS charges, the URFC stack consumes water from the water storage tank and produces oxygen and hydrogen, which are stored in the gas storage tanks. During the discharge of the URFCS, gas is withdrawn from the gas storage tanks, reacted within the URFC stack, and the resultant water is stored within the water storage tank. During both URFCS charging and discharging, the waste heat generated by the URFC stack is carried to the surface of the gas storage tanks via loop heat pipes (LHPs). Details of the operating principles of this system have previously been described (ref. 1).

One of the key features of the system shown in figure 1 is the hydrogen and oxygen gas storage tanks. Each of these tanks is illustrated having an LHP wrapped several times around its outside diameter. These LHPs are part of an overall LHP heat-rejection system.

LHPs passively transfer heat by utilizing the working fluid's heat of vaporization as an energy transport mechanism. An LHP, shown in figure 2, consists of four components connected in a fluidic loop: a compensation chamber, an evaporator, a condenser, and connective tubing.

Starting from the compensation chamber, the liquid working fluid enters the evaporator and uses the thermal energy added to the system to change from a liquid to a vapor. The evaporating surface within the evaporator that separates the liquid phase from the vapor phase consists of a fine capillary structure. When this capillary structure is filled with liquid it is resistant to vapor flow, and therefore as the liquid evaporates, the vapor preferentially flows out of the evaporator outlet rather than through the capillary structure and out through the liquid inlet. As liquid is removed from the capillary structure, more liquid is drawn in by the structure's capillary forces. The expansion of fluid volume on the vapor side of the evaporator and the capillary suction force on the liquid side of the evaporator are the driving forces that move the working fluid around the LHP. The vapor from the evaporator moves through the connective

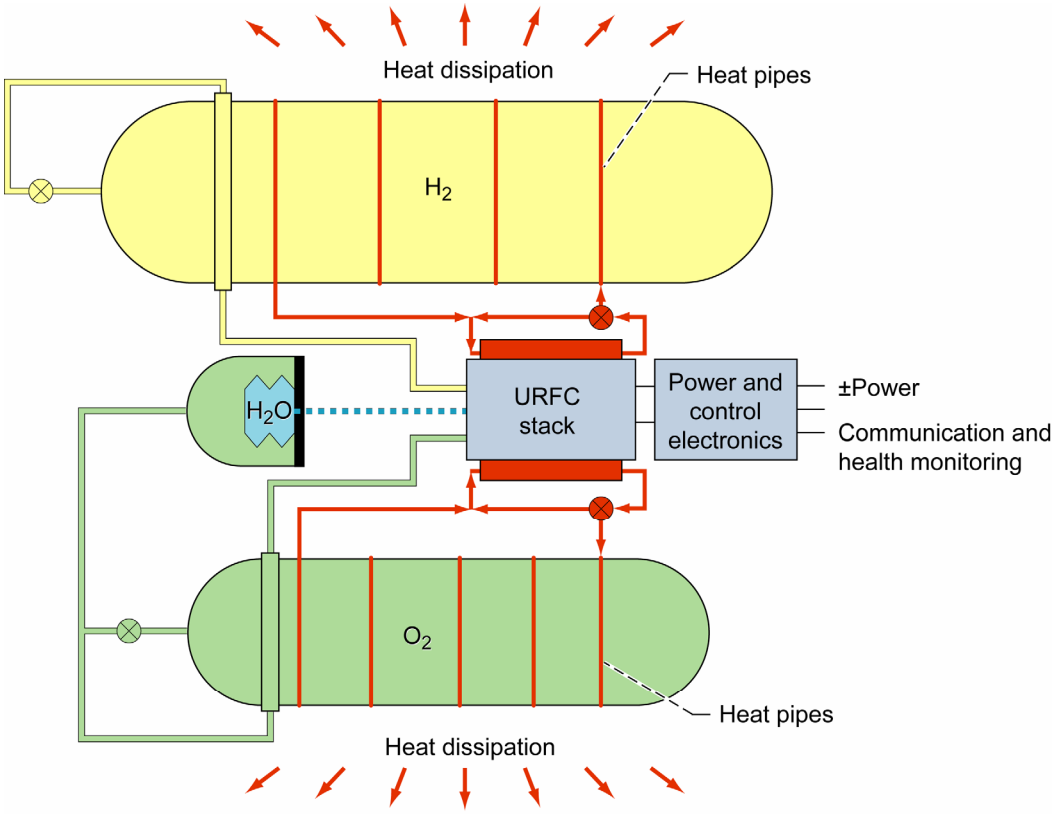

Figure 1.—Unitized regenerative fuel cell (URFC).

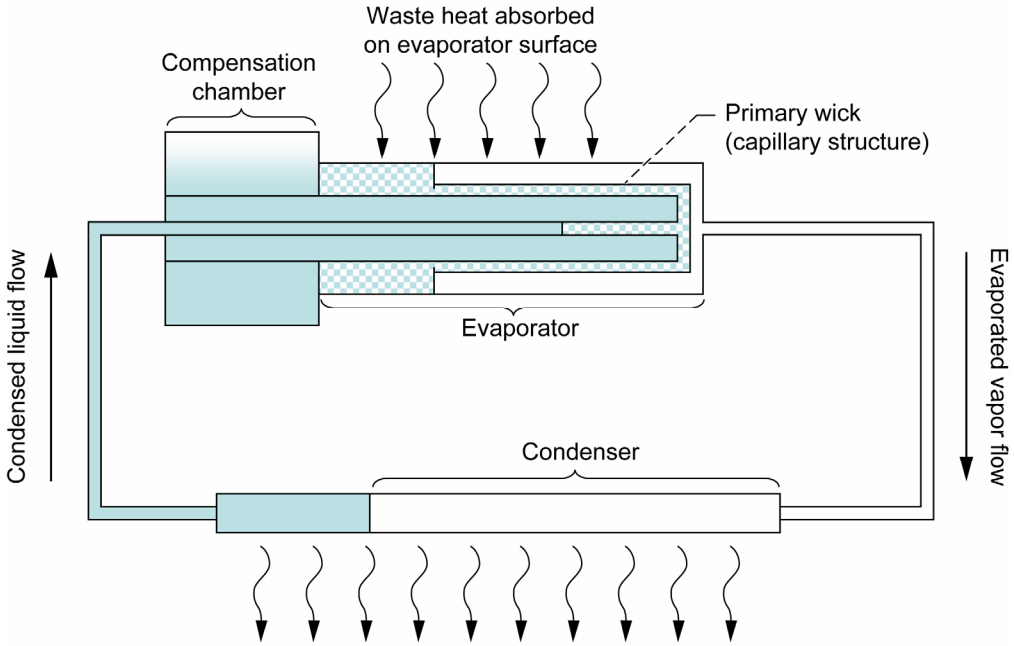

Figure 2.—Loop heat pipe (LHP).

tubing, which is wound around the outside diameter of each of the gas storage tanks to form the condenser. The condenser tubing is cooled by the radiant heat rejection occurring on the surface of the gas storage tanks. Since the walls of the condenser are at a lower temperature than the vapor, the vapor condenses. The LHP pumping forces described earlier drive the working fluid, now a liquid, back into the compensation chamber. The compensation chamber functions as an accumulator and fluid reservoir. For more information regarding the description of the LHP and its operating characteristics, the reader is referred to references 3 and 4.

Test Articles

One of the key considerations in the development of the test articles was the storage tank wall material. Besides having good strength characteristics, it was critical to have good thermal conductivity, so that heat absorbed from the heat pipes would be uniformly spread without requiring numerous LHP coils. Carbon fibers embedded within an epoxy matrix have been used to construct lightweight tanks because of their very high strength to mass, and some of these carbon fibers also have remarkable thermal conductivity. Table I lists the tensile strength, elastic modulus, and thermal conductivity of several commonly used metals, carbon fibers, as well as the carbon fiber/epoxy prepreg from which the test articles were made.

From the values listed in table I, it is apparent that carbon fibers with their high strength and low density make ideal materials for tank construction. The pitch-based carbon fibers, although not as strong as the PAN-based fibers, have thermal conductivities 2 to 3 times that of copper.

TABLE I.—MECHANICAL AND THERMAL PROPERTIES OF SELECTED MATERIALS[a]

Material[b]	Tensile strength, Mpa	Elastic modulus, Gpa	Thermal conductivity, W-m/K	Density, g/cm^3
Stainless steel 316	515	193	16.2	8
Copper	221 to 455	<125	393.4	8.96
Aluminum 6061–T6	310	<72	167	2.7
Titanium	152	103	22.5	4.51
UHM carbon (PAN)	3800	590	18	1.9
UHS carbon (PAN)	7000	290	160	1.8
UHM carbon (pitch)	2200	895	640	2.2
UHK carbon (pitch)	2200	830	1100	2.2
RS–3C/K800 5 mil	1300	470	391	1.2

[a]From references 5 to 8.
[b]UHM is ultrahigh modulus; UHS, ultrahigh strength; and UHK, ultrahigh conductivity.

The RS–3/K800 carbon epoxy prepreg[1] provides a good combination of both high strength and excellent thermal conductivity. Other carbon epoxies were available with still higher thermal conductivities, but these were much higher in cost, and a judgment was made that the RS–3/K800 material was a reasonable compromise that could prove the feasibility of the gas storage tank/radiator concept. It was planned to have two gas storage tank test articles made from the RS–3/K800 carbon epoxy.

The test coupons made were 30.5-cm (12-in.) squares with a single straight section of LHP tubing. The purpose of the coupons was to investigate different fabrication methods as well as the heat spreading performance. The LHP tubing was charged with ammonia and tested at Thermacore, Inc.[2] The choice of

[1] Material obtained from Material Innovations, Inc., 2200 Amapola Court, Suite 101, Torrance, CA 90501.
[2] Thermacore, Inc., 780 Eden Rd, Lancaster, PA 17601.

ammonia as the working fluid was based on the anticipated operating temperature range for the test. The optimal choice for a working fluid would ultimately be determined based upon application requirements. The purpose of these tests was to determine the feasibility of using gas storage tanks as heat-radiating surfaces and not to determine the working fluid for such a system. Figure 3 shows three of the coupons prior to being thermal vacuum tested. Figure 4 shows the measured heat distribution pattern of one of the tested coupons.

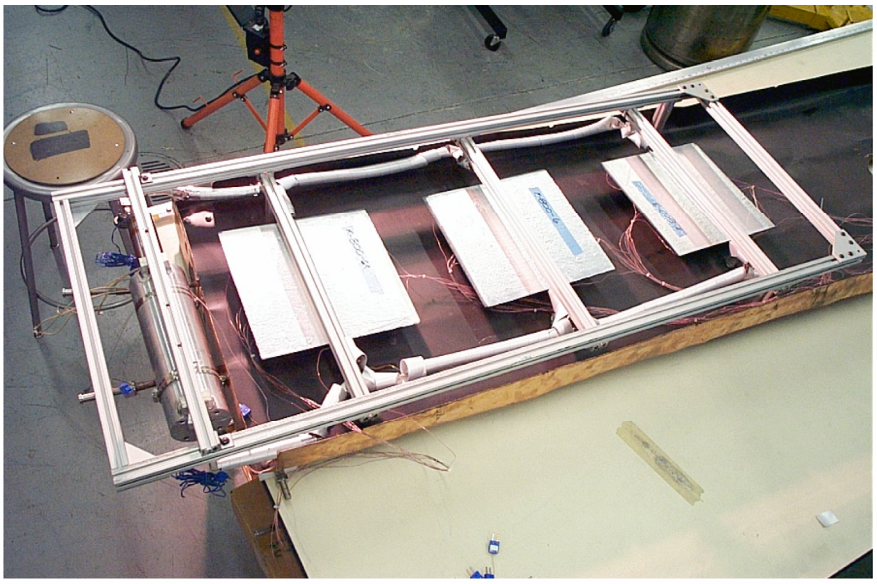

Figure 3.—LHP coupon testing.

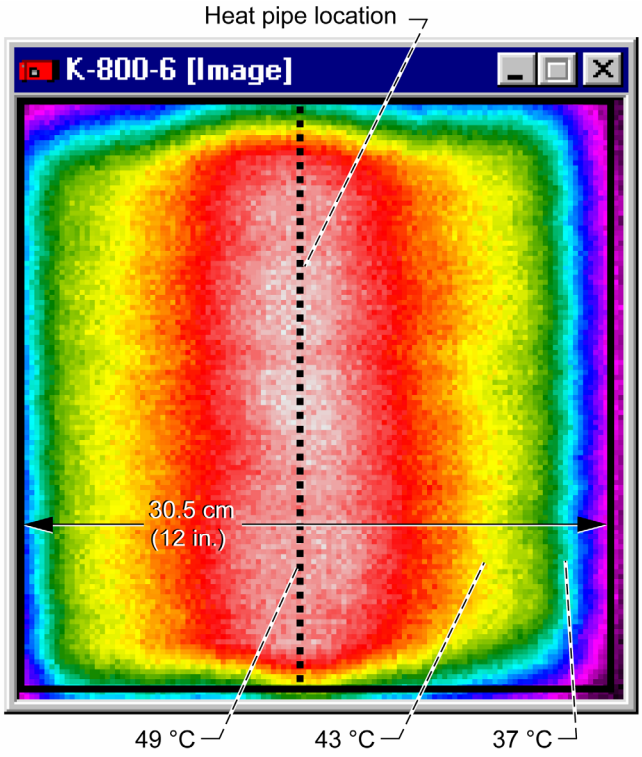

Figure 4.—LHP coupon temperature distribution.

From the coupon fabrication and testing it was determined to bond the LHP tubing to the outside of the completed tank structure rather than embed the LHP tubing within the wall structure. It was also decided to wrap the coils with 15.2 cm (6.0 in.) of space between coils, (i.e., a 6-in. pitch) to minimize temperature differentials on the tank surface and to minimize the number of LHP coils needed to distribute the heat.

The two tank test articles were originally to be fabricated using the 5-mil RS–3/K800 carbon epoxy material with an aluminum foil liner. The vendor selected to fabricate the tanks with RS–3/K800 carbon epoxy failed to fabricate a leak-proof tank because the end boss material leaked severely. The cause of this leakage was not the RS–3/K800 material. Because of these fabrication problems, an alternative plan was adopted, and two commercially available, epoxy fiberglass tanks rated by the Department of Transportation (DOT) and having seamless aluminum liners were purchased from Carleton Technologies, Inc.[3]

The heat pipes were attached to the outside using Hysol EA 9394 epoxy[4] and the RS–3/K800 epoxy/carbon material. The RS-3/K800 carbon epoxy was applied in approximately 5.1-cm (2.0-in.) strips that were run perpendicular to the heat pipes. Two overlapping layers (a total of 0.254 mm (0.010 in.) of thickness) of RS–3/K800 were applied in this fashion. One final strip of RS–3/K800 was applied directly over the heat pipe coil and was aligned in the same direction as the heat pipe. This layer was applied primarily to cover the cracks in the epoxy carbon that developed during the bending of the carbon epoxy over the heat pipe tubing radii. Considerable difficulty was encountered in attempting to get the carbon epoxy to follow the curvature over the top of each heat pipe loop because the carbon epoxy material at room temperature is quite brittle. Working with the material warmed to 35 to 40 °C made it more pliable and significantly reduced broken fibers. To cure the epoxy, each test article was placed within a vacuum bag and placed into an oven to cure at 150 °C (300 °F) for 6 h. The vacuum was maintained within the vacuum bag during the entire cure process. Figures 5 and 6 show the fabricated tanks.

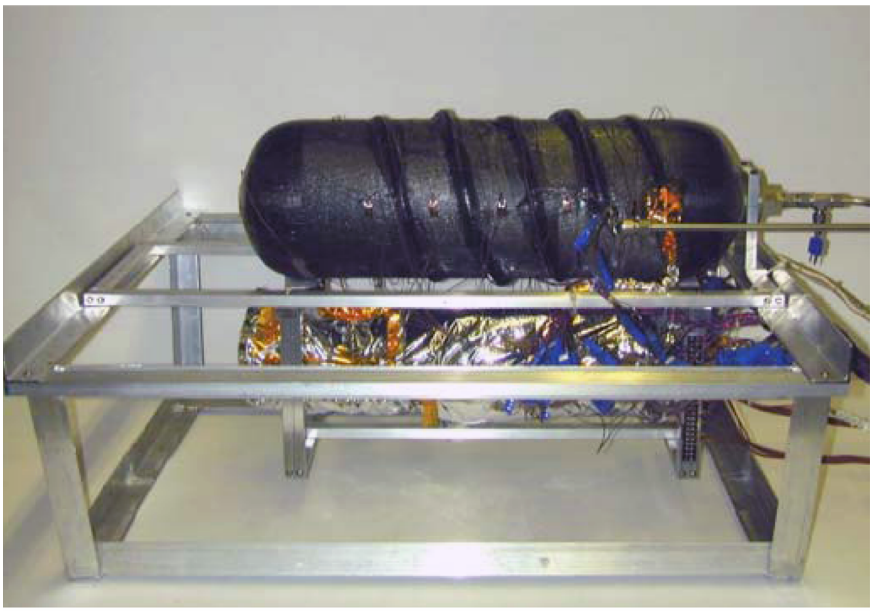

Figure 5.—Oxygen tank with integral heat pipe.

[3] Carleton Technologies, Inc., 504 McCormick Drive, Glen Burnie, MD 21061.
[4] Loctite Aerospace, Henkel Corporation, 2850 Willow Pass Road, P.O. Box 312, Bay Point, CA 94565-0031, Phone: 925–458–8000.

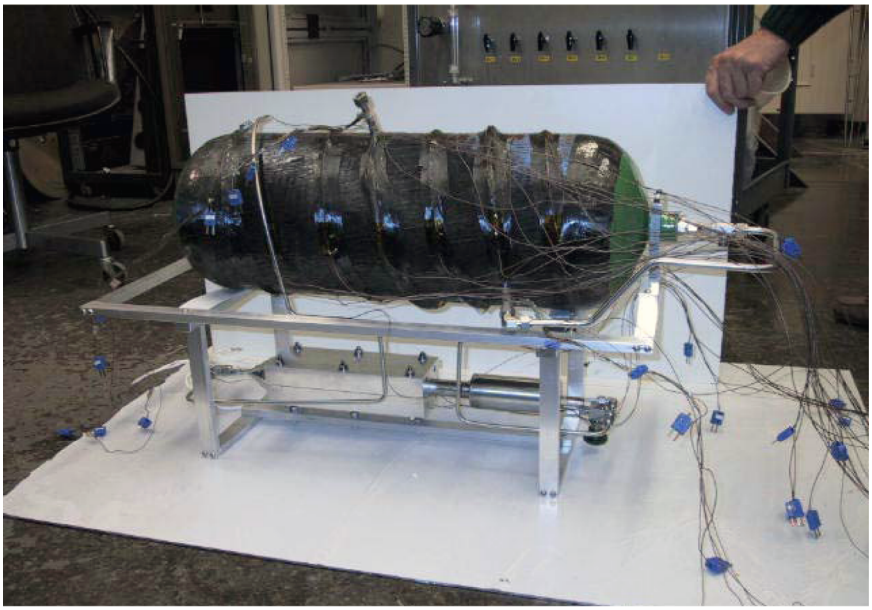

Figure 6.—Hydrogen tank with integral heat pipe.

The smaller of the two tanks, which represented the oxygen tank of a URFCS, was approximately 13.1 liters (800 in^3) in volume with a diameter of 19.3 cm (7.6 in.) and a length of 64.5 cm (25.4 in.). Its weight before applying the carbon epoxy material was approximately 6.5 kg (14.3 lb). Three and one-third LHP coils were applied (approximately 208 cm (82 in.) in length). The number of coils was selected based on the 15.2 cm (6.0 in.) of space between coils, (i.e., a 15.2-cm or 6-in. pitch). The 3 1/3 coils were sufficient to wrap the cylindrical portion of the tank. The heat pipe tubing was 316 stainless steel, with dimensions of 2.54 mm (0.1 in.) o.d. and 0.25 mm (0.01 in.) wall thickness. The tank was wrapped with composite material over a surface area of approximately 0.40 m^2 (620 in^2) for the oxygen tank. The ratio of wrapped surface area to the length of LHP was about 0.192 m^2 (297.6 in^2) per meter length of LHP. Also attached was a regenerative gas dryer tube that was to be used in subsequent experiments involving the dehumidification and rehumidification of O_2 gas as it flows to and from the gas storage tank.

The larger of the two tanks, which represented the hydrogen tank of a URFCS, was approximately 24.6 liters (1500 in^3) in volume with a diameter of 23.5 cm (9.25 in.) and a length of 75.2 cm (29.6 in.). Its mass before applying the epoxy/carbon was approximately 7.85 kg (17.3 lb). Three and one-third LHP coils were applied (approximately 251.5 cm (99 in.) in length). The number of coils was selected based on the 15.2 cm (6.0 in.) of space between coils, (i.e., a 15.2-cm or 6-in. pitch). The 3 1/3 coils were sufficient to wrap the cylindrical portion of the tank. The heat pipe tubing was 316 stainless steel, with dimensions of 2.54 mm (0.1 in.) o.d. and 0.25 mm (0.01 in.) wall thickness. The tank was wrapped with composite material over a surface area of approximately 0.49 m^2 (759.5 in^2) for the hydrogen tank. The ratio of wrapped surface area to the length of LHP was about 0.195 m^2 per meter length of LHP.

The completed tanks were shipped to Thermacore, Inc., for the addition of the LHP evaporators, compensation chambers, and other connective tubing. Thermacore, Inc., charged the LHPs with ammonia and did an initial check of the LHP operation of both tanks before shipping the completed assemblies to NASA Glenn. The completed assemblies were instrumented with thermocouples and mounted within aluminum frames (shown in figs. 5 and 6) for easy insertion into the thermal vacuum test chamber.

Experiment

The purpose of the experiment was threefold: first to determine how well the heat from the evaporator was conducted to the tank and spread across the surface of the tank through the carbon epoxy material and second to determine how well the tank functioned as a heat radiating surface. Lastly, appropriate measurements of key thermal characteristics will be needed to model the observed performance so that predictions of flight performance can be made.

Each of the tanks was tested individually within the same thermal vacuum chamber, and then both tanks were inserted into the vacuum chamber and tested simultaneously. Rather than use oxygen and hydrogen for the testing, nitrogen was used to simulate oxygen and helium was used to simulate hydrogen. This was done to reduce safety concerns related to handling pressurized combustible gases. The difference in the physical properties between the oxygen and nitrogen and between the hydrogen and helium is thought not to affect the performance of the tanks as radiators. Results discussed later in this paper show no significant difference in performance between the smaller tank, which used nitrogen and the larger tank which used helium, and the differences in physical properties between nitrogen and helium are greater than the differences between either oxygen and nitrogen or between helium and hydrogen.

The vacuum chamber is cylindrically shaped with a 1-m i.d. and a length of about 1.5 m. The vacuum chamber cold wall covered all interior surfaces of the chamber except the front access cover. The chamber was routinely operated at less than 2.0×10^{-6} torr, and the cold wall was kept at –100 to –120 °C. The placement of each tank within the vacuum chamber is illustrated in figure 7. Each tank was oriented with its long axis parallel to the long axis of the vacuum chamber. The evaporator and compensation chamber for each of the test articles were mounted directly below the tanks. This placement ensured that any ammonia liquid would drain to the compensation chamber of the LHP. The fluid-driving forces of the LHP as described earlier are inherently gravity independent, yet while testing in a gravitational environment, the pooling of the working fluid in portions of the LHP other than the evaporator and compensation chamber could create startup transients. It was felt these transients could lengthen the needed testing time and possibly complicate the interpretation of the results.

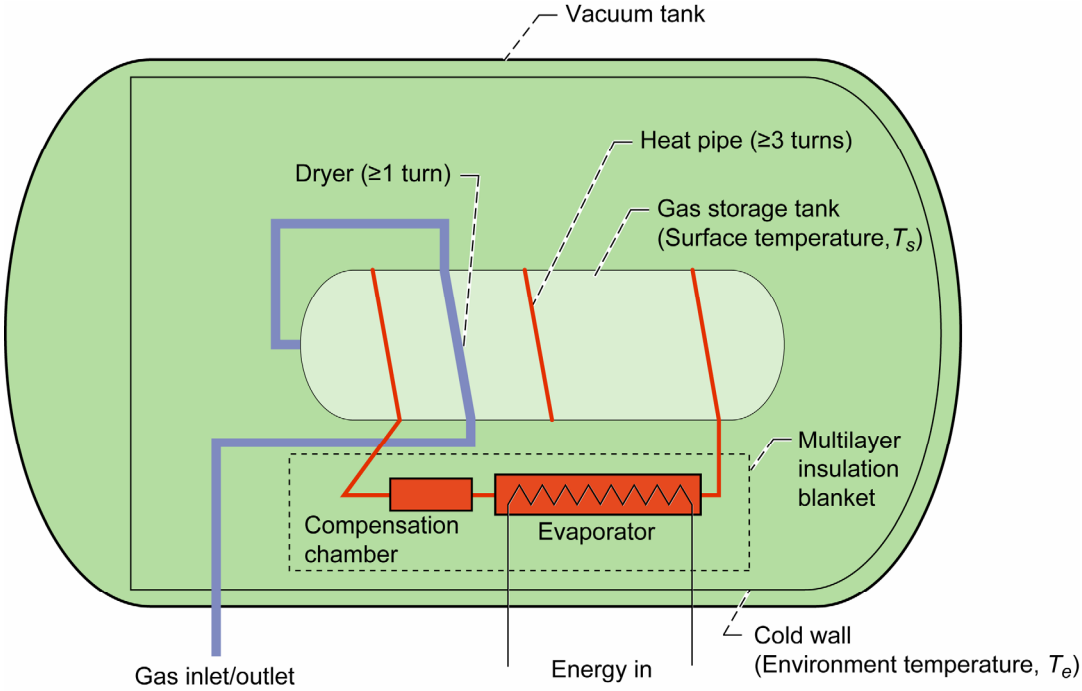

Figure 7.—Test article placement in vacuum chamber.

The evaporators for this test were aluminum, each with four imbedded cartridge heaters to simulate the RFC stack waste heat load. The evaporator, compensation chamber, and connecting tubing for each LHP were wrapped in a four-layer thermoreflective aluminized Mylar[5] blanket to minimize the heat dissipation directly to the vacuum chamber cold wall. This was done so that the heat dissipation from the LHP would predominantly come from the heat radiation from the tank surface. The dedicated dc power supply for each test article evaporator would be set at the appropriate power level in a constant current mode to achieve the proportional power level required. For the analysis it was assumed that all of the electrical power from the dc power supply was dissipated from the tank surface.

Results

The surface temperature distribution, thermal emissivity, specific heat, and mass of attached LHPs were determined for each gas storage tank.

Surface Temperature Distribution

The oxygen tank was tested at three different waste heat levels using nitrogen as the test gas. Figure 8 shows the surface temperatures measured at one of those heat levels.[6] The figure shows that the heat radiating surface has for the most part a temperature range of 0.6 to 10.9 °C. One area shown on these figures falls outside this range. This area has a temperature of –22.5 °C. Data from other tests showed this particular area on the oxygen tank to have a much lower temperature than other adjoining radiator areas, indicating significantly poorer heat conductance to this area. The reason for this is not known, but it is suspected that the heat conductive carbon fibers may have broken in the bended area directly over the heat pipe during the application of the carbon composite layers.

The hydrogen tank was tested at three different waste heat levels using helium as the test gas. Figure 9 shows the surface temperatures measured at one of those heat levels.[7] The temperature distribution across the hydrogen tank was 3 to 20 °C. Some temperature distribution was expected because of the dissipation of heat along the flow path of the heat pipe and dryer tube. The lowest temperatures in this range were at the end of the flow path of the heat pipe, where lower temperatures would be expected.

Table II lists the average tank surface temperature recorded and the waste heat power level for the tests conducted on both size tanks.

TABLE II.—OXYGEN AND HYDROGEN TANK THERMAL RESULTS

Test gas[a]	Waste heat power, W	Tank surface avg. temperature, °C	Tank surface temperature range, °C	Cold wall avg. temperature, °C	Date of test
Nitrogen	16.6	–66	–81 to –54	–94	27 Oct. 2003
Nitrogen	42	–39	–61 to –18	–103	28 Oct. 2003
Nitrogen	86	1.7	–22.5 to 11	–91	17 Oct. 2003
Helium	60	–27.3	–34 to –20	–100	18 Nov. 2003
Helium	90	–8.4	–8 to 4	–103	02 Dec. 2003
Helium	125	10.9	4 to 20	–103	21 Nov. 2003

[a]Nitrogen was the test gas for the oxygen tank, and helium was the test gas for the hydrogen tank.

[5] DuPont, Wilmington, DE.
[6] Test data for the nitrogen tank emissivity calculations came from tests conducted on 17, 27, and 28 October 2003.
[7] Test data for the helium tank emissivity calculations came from tests conducted 18 and 21 November 2003.

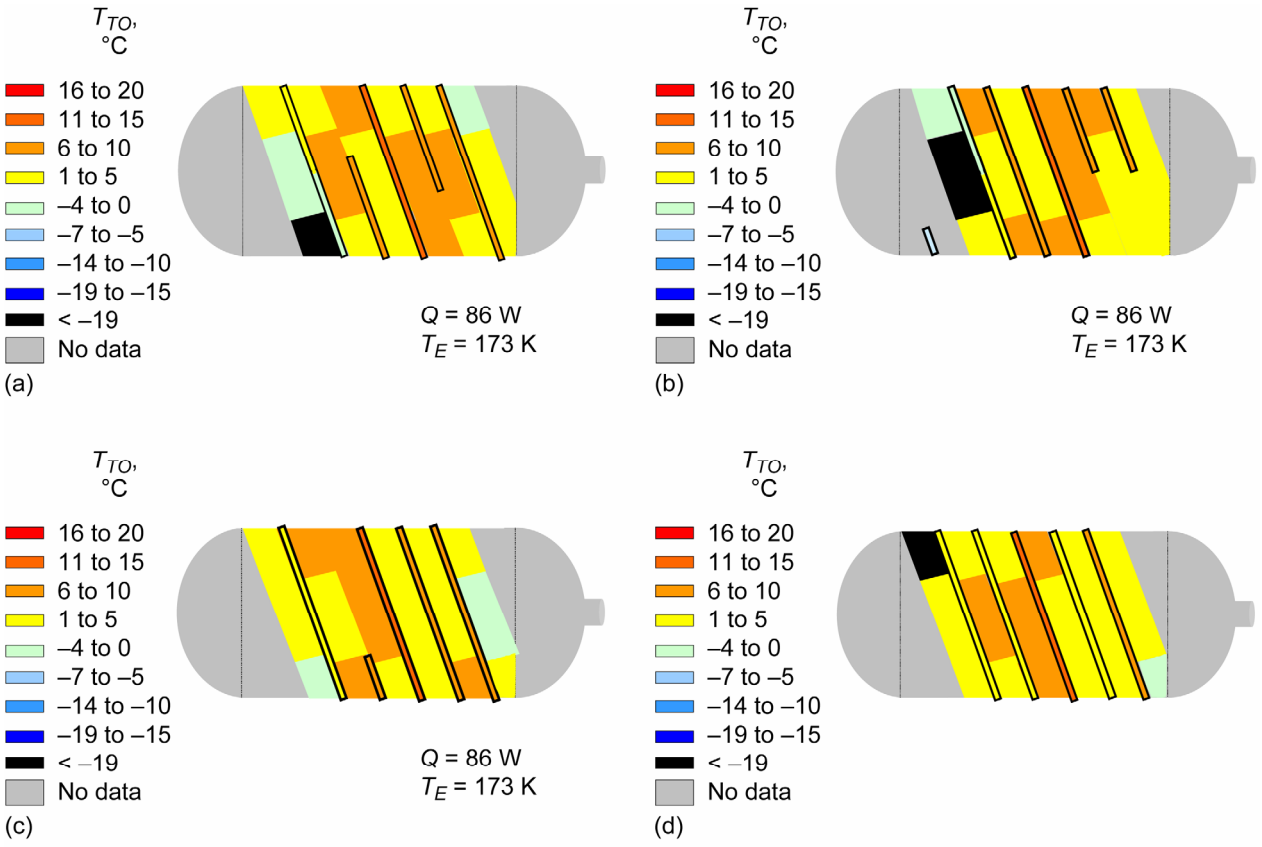

Figure 8.—Oxygen tank surface temperature, T_{TO}. Q is heat radiation, T_E is environment temperature. Tests run Oct. 17, 2003. (a) Top view. (b) Left side view. (c) Right side view. (d) Bottom view.

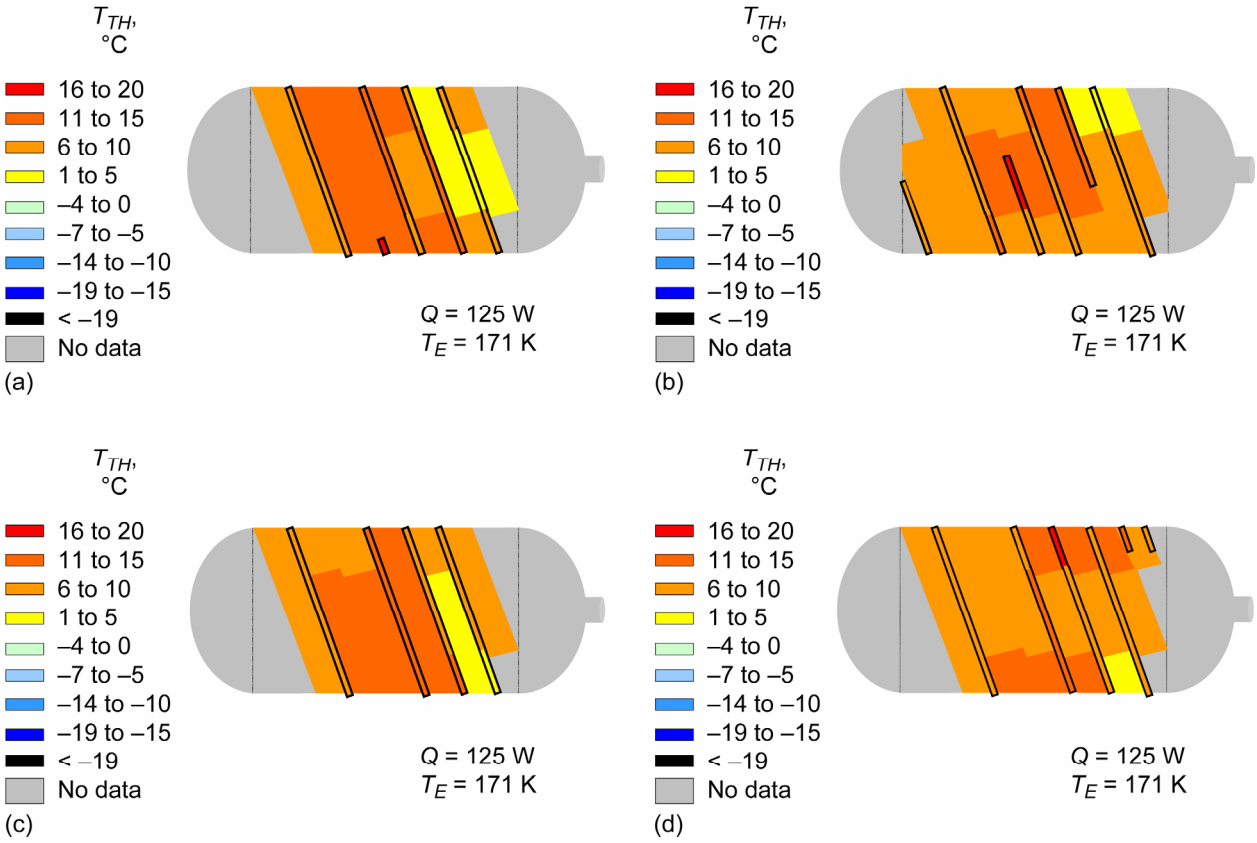

Figure 9.—Hydrogen tank surface temperature, T_{TH}. Q is heat radiation, T_E is environment temperature. Tests run Nov. 21, 2003. (a) Top view. (b) Left side view. (c) Right side view. (d) Bottom view.

Emissivity

The Stefan-Boltzmann Law states that

$$Q = e\sigma A\left(T^4 - T_E^4\right) \tag{1}$$

where

Q	heat radiation, W
e	emissivity, dimensionless
A	heat radiation area, m^2
σ	5.6703×10^{-8} $W/m^2/K^4$
T	temperature of radiating body, K
T_E	temperature of environment, K

For this test it was assumed that the heat input was equivalent to the heat dissipated from the surface of each tank. As was mentioned earlier, the evaporator, compensation chamber, and all the connecting tubing were wrapped with insulation to prevent heat loss directly from these components. Rewriting equation (1) for the oxygen and hydrogen tanks,

$$Q_O = e_O \sigma A_O \left(T_{TO}^4 - T_E^4 \right) \tag{2}$$

$$Q_H = e_H \sigma A_H \left(T_{TH}^4 - T_E^4 \right) \tag{3}$$

where

Q_O heat radiation from the oxygen tank, W
Q_H heat radiation from the hydrogen tank, W
e_O emissivity of oxygen tank, dimensionless
e_H emissivity of hydrogen tank, dimensionless
A_O surface area of oxygen tank, m^2
A_H surface area of hydrogen tank, m^2
T_{TO} surface temperature of oxygen tank, K
T_{TH} surface temperature of hydrogen tank, K

By plotting the radiated heat versus the average surface temperature to the fourth power, the resultant curve should approximate a straight line.

Figure 10 plots this data (from table II), and the resultant curves were approximately straight lines. Since the radiating surface area and Boltzmann constant were known values, an estimation of the emissivity for each tank could be made.

Table III contains the calculated emissivity for each tank.

Table IV lists the published values of emissivity for other materials. These published values compare well to the calculated emissivity values of the two tanks whose surfaces were covered with black carbon fibers and epoxy.

TABLE III.—CALCULATED EMISSIVITIES OF OXYGEN AND HYDROGEN TANKS

Storage tank	Linear slope, W/K^4	Linear intercept, $W\text{-}m^4\text{-}K^4$	Radiative surface area, m^2	Boltzmann constant, $W/m^2/K^4$	Calculated emissivity
Oxygen	1.92E–08	–17.40	0.40	5.67E–08	0.86
Hydrogen	2.38E–08	–26.50	.49	5.67E–08	.86

TABLE IV.—EMISSIVITY VALUES OF SELECTED MATERIALS[a]

Material	Emissivity
Carbon rough plate	0.79 to 0.81
Carbon lampblack	0.78 to 0.84
Black shiny lacquer	0.875
Flat black lacquer	0.96 to 0.98
Aluminum plate	0.09

[a]From reference 9.

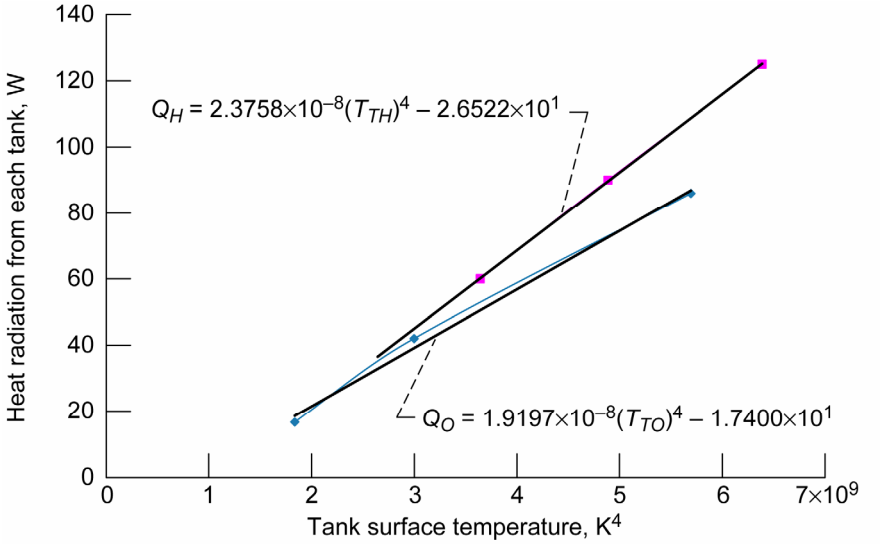

Figure 10.—Oxygen and hydrogen tank heat radiation (Q_O and Q_H) as function of respective surface temperature, T_{TO} and T_{TH}.

Specific Heat

Temperature decay tests were run to experimentally determine the specific heat capacity of each tank.[8,9]

After a steady-state tank surface temperature was established with a given energy input, the power was turned off and the tank allowed to cool. The rate at which it cooled allowed the specific heat capacity to be estimated.

An assumption was made that the heat radiated from the oxygen tank surface was the combined sensible heat loss from both the oxygen tank and the portions of the LHP that were external to the oxygen tank. Similarly, an assumption was made that the heat radiated from the hydrogen tank surface was the combined sensible heat loss from both the hydrogen tank and the portions of the LHP that were external to the hydrogen tank. These assumptions were made because evaporation would continue inside the evaporators, even though heat input onto the surface of the evaporator had stopped. The cooling effect of this evaporation would be reflected in the drop in the evaporator and compensation chamber temperature. Writing the radiation heat loss in terms of the resultant sensible heat losses,

$$Q_O = -\left(M_{TO} C_{P,O} \frac{\mathrm{d}T_{TO}}{\mathrm{d}t} + M_{HO} C_{P,HO} \frac{\mathrm{d}T_{HO}}{\mathrm{d}t} \right) \tag{4}$$

$$Q_H = -\left(M_{TH} C_{P,H} \frac{\mathrm{d}T_{TH}}{\mathrm{d}t} + M_{HH} C_{P,HH} \frac{\mathrm{d}T_{HH}}{\mathrm{d}t} \right) \tag{5}$$

where

M_{TO} mass of the oxygen tank, kg
M_{TH} mass of the hydrogen tank, kg
M_{HO} mass of the oxygen heat pipe, kg

[8]Data for the oxygen tank specific heat calculations came from the 4 November 2003 test, 11:02:02 a.m. through 1:47:11 p.m.

[9] Data for the hydrogen tank specific heat calculations came from tests conducted 15 December 2003.

M_{HH} mass of the hydrogen heat pipe, kg
$C_{P,O}$ specific heat of the oxygen tank, kJ/kg/K
$C_{P,H}$ specific heat of the hydrogen tank, kJ/kg/K
$C_{P,HO}$ specific heat of the oxygen heat pipe, kJ/kg/K
$C_{P,HH}$ specific heat of the hydrogen heat pipe, kJ/kg/K
dT_{TO}/dt temperature change rate of O_2 tank, K/h
dT_{TH}/dt temperature change rate of H_2 tank, K/h
dT_{HO}/dt temperature change rate of O_2 heat pipe, K/h
dT_{HH}/dt temperature change rate of H_2 heat pipe, K/h

Rewriting equations (4) and (5) and solving for the specific heat capacity of the gas storage tanks,

$$C_{P,O} = -\frac{\left(Q_O + M_{HO} C_{P,HO} \frac{dT_{HO}}{dt}\right)}{\left(M_{TO} \frac{dT_{TO}}{dt}\right)} \tag{6}$$

$$C_{P,H} = -\frac{\left(Q_H + M_{HH} C_{P,HH} \frac{dT_{HH}}{dt}\right)}{\left(M_{TH} \frac{dT_{TH}}{dt}\right)} \tag{7}$$

Figure 11 illustrates data obtained from a temperature decay test of the oxygen tank,[8] and figure 12 shows data obtained from a temperature decay test of the hydrogen tank.[9]

Using the emissivity experimentally determined for each tank in earlier testing as well as the known values for the mass of each tank and the mass of each heat pipe, the specific heat was determined for each tank using equations (6) and (7). The average specific heat of the heat pipe was a weighted average based

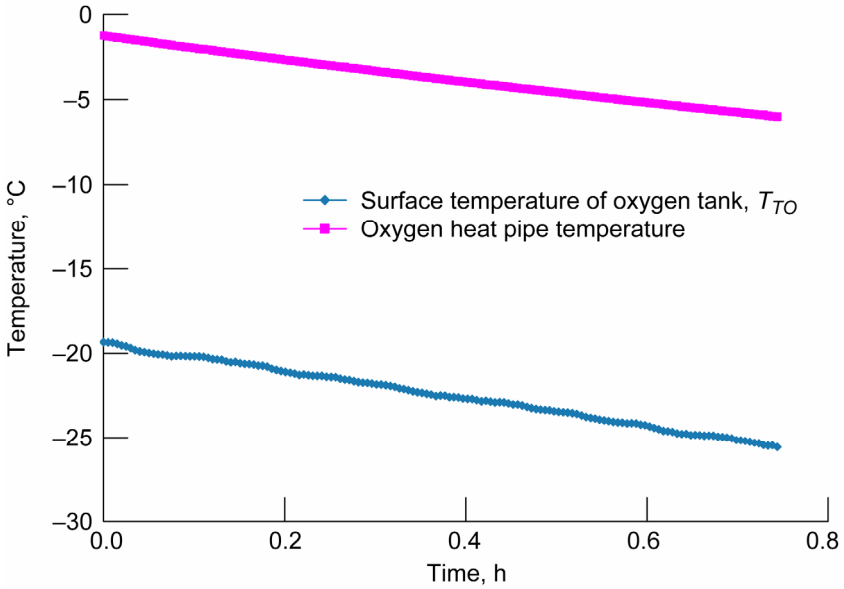

Figure 11.—Oxygen tank temperature decay. Environment temperature T_E is 180 K. Tests run Oct. 16, 2003.

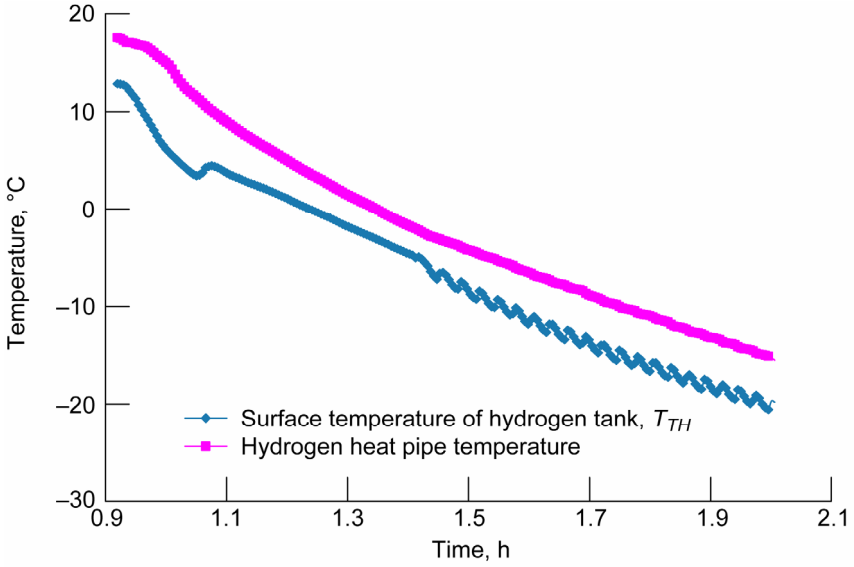

Figure 12.—Hydrogen tank temperature decay. Environment temperature T_E is 167 K. Tests run Dec. 15, 2003.

on the different materials used to construct the heat pipe. Table V is a listing of the data points taken from figures 11 and 12, and the calculations done to determine the average specific heat of the oxygen tank and the hydrogen tank. The measured average specific heat of the oxygen tank was 2.81 kJ/kg/K, and the measured average specific heat of the hydrogen tank was 1.13 kJ/kg/K. The specific heat values of other materials are listed in table VI for comparison with these.

TABLE V.—CALCULATED TANK SPECIFIC HEAT[a]

Time, h	Tank temp., K	HP temp., K	Cold wall temp., K	Tank mass, kg	HP mass, kg	Tank dT_{TO}/dt, K/h	HP dT_{TO}/dt, K/h	Tank heat loss, W	HP heat loss, W	HP avg. specific heat, kJ/kg/K	Tank specific heat, C_P, kJ/kg/K
Oxygen tank											
0.0	254	272	183	6.5	8.8	–8.31	–7.39	58.8	–17.0	0.941	2.78
0.1	253	271	182	6.5	8.8	–8.77	–6.67	58.4	–15.4		2.71
0.2	252	270	178	6.5	8.8	–7.73	–6.91	59.0	–15.9		3.09
0.3	251	270	181	6.5	8.8	–8.49	–6.47	56.6	–14.9		2.72
0.4	250	269	180	6.5	8.8	–7.70	–6.02	56.1	–13.9		3.04
0.5	250	268	180	6.5	8.8	–8.26	–6.03	55.0	–13.9		2.76
0.6	249	268	179	6.5	8.8	–8.96	–5.66	54.9	–13.0		2.59
0.7	248	267	177	6.5	8.8			54.5			
Average C_{PO} = 2.81											
Hydrogen tank											
1.0	279	288	169	7.9	3.0	–20.90	–56.10	102.7	–42.2	0.904	1.33
1.1	277	282	170	7.9	3.0	–30.40	–44.50	98.7	–33.5		0.98
1.2	274	278	169	7.9	3.0	–30.60	–37.20	94.1	–28.0		0.99
1.3	271	274	168	7.9	3.0	–25.88	–29.41	89.8	–22.1		1.20
1.4	268	271	168	7.9	3.0	–37.38	–25.60	85.7	–19.3		0.81
1.5	265	269	166	7.9	3.0	–25.65	–23.84	81.0	–17.9		1.13
1.6	262	266	161	7.9	3.0	–26.25	–22.16	78.7	–16.7		1.08
1.7	259	264	163	7.9	3.0	–19.67	–22.83	74.2	–17.2		1.33
1.8	258	262	166	7.9	3.0	–20.96	–20.87	71.4	–15.7		1.22
1.9	256	260	170	7.9	3.0	–18.93	–20.98	67.1	–15.8		1.24
2.0	254	258	173	7.9	3.0			63.8			
Average C_{PH} = 1.13											

[a]HP is heat pipe.

TABLE VI.—SPECIFIC HEAT VALUES OF SELECTED MATERIALS[a]

Material	Specific heat, kJ/kg/K
Polyethylene	2.3
Polypropylene	1.9
Polyvinyl chloride	1.3 to 1.7
Teflon[b]	1.0
Cast epoxy fiber glass filled	0.8
Aluminum	0.92 to 0.96
Fiber glass chopped strand mat	1.3 to 1.4
Stainless steel	0.50
Water	1.0

[a]From reference 10.
[b]DuPont, Wilmington, DE.

The specific heat value determined for the hydrogen tank is of a magnitude similar to the several plastics and fiber glass, but higher than a dense metal like stainless steel. The specific heat determined for the oxygen tank is higher than one would expect for this material, and higher than the hydrogen tank, which was constructed of similar materials. The oxygen heat pipe mass is larger than the oxygen tank itself, which may have contributed to inaccuracies.

URFCS Radiator Mass Analysis

The mass of the LHP that was attached to each tank was analyzed, and a mass per unit length of heat pipe was determined (table VII). From the coil pattern on each tank it was then possible to calculate the mass of the radiator per unit area.

TABLE VII.—URFCS RADIATOR MASS ANALYSIS

Heat pipe unit length, cm	1
Heat pipe tube o.d., cm	0.25
Heat pipe tube i.d., cm	0.20
Material cross-sectional area	
Epoxy area, cm^2	3.23×10^{-2}
Tube area, cm^2	1.82×10^{-2}
Composite area, cm^2	3.87×10^{-1}
Material volume per centimeter of heat pipe length	
Epoxy volume, cm^3	3.23×10^{-2}
Tube volume, cm^3	1.82×10^{-2}
Composite volume, cm^3	3.87×10^{-1}
Heat pipe material densities	
Epoxy density, g/cm^3	1.36
Tube density, g/cm^3	7.76
Composite density, g/cm^3	1.236
Heat pipe masses per unit length	
Epoxy mass, g	4.39×10^{-2}
Tube mass, g	1.42×10^{-1}
Composite mass, g	4.78×10^{-1}
Radiator mass/inch, g/cm	**0.66**
Radiative area/tube length, cm^2/cm	**19.35**
Radiator weight/area, g/cm^2	**0.03**
Radiator weight/area, kg/m^2	**0.34**

The technique used to construct the URFCS radiator resulted in a mass per unit area of 0.34 kg/m^2. The International Space Station (ISS) photovoltaic radiator (PVR) uses two-sided radiator panels that have a mass per unit area of 2.75 kg/m^2. When the masses of the fluid loop and deployment mechanism are added, this ratio increases to 8.8 kg/m^2 (ref. 11).

An analysis of the radiator mass for the Jupiter Icy Moons Orbiter mission resulted in a radiator system that had an estimated mass of 5 kg/m^2 when the mass of the pumped coolant loop and deployment mechanism was added to the radiator panels (ref. 12).

The following illustrates the potential mass savings for 10-kW URFCS: Assuming a 50-percent fuel cell efficiency for this tank, the waste heat that would have to be dissipated during discharge would be approximately 10 kW. At a heat rejection temperature of about 353 K and an environmental temperature of 173 K, and assuming an emissivity of 0.86, the required heat-radiating area is approximately 1.4 m^2/kW; for a 10-kW heat load, this is approximately 14 m^2 of radiator surface. Assuming a separate radiator would contribute 5 kg/m^2, 70 kg would be the mass of such a radiator system, whereas the added mass to the gas storage tank by LHPs to provide the heat-radiating function would be only 4.8 kg.

Conclusions

The gas storage tanks make an excellent substrate for mounting a heat-pipe-based radiator. The resulting combination gas storage tank-radiator performs well and is extremely lightweight. The mass added to the gas storage tank in order to mount the radiator is about one-fifteenth the mass of a comparably sized, flight-weight space radiator. Since the heat pipe system contains no pump, there is less parasitic power and no moving components to fail, which makes the URFCS more energy efficient and less prone to component failure.

Although this radiator development was envisioned for a fuel cell application, the basic concept of using large surface area pressure vessels as heat radiating surfaces has applicability to pressure vessels used for propellant storage or gas storage for environmental control. Likewise, heat pipes could perform the same function being attached to any suitably sized structure present in a system.

References

1. Burke, Kenneth A.: Unitized Regenerative Fuel Cell System Development. NASA/TM—2003-212739, 2003. http://gltrs.grc.nasa.gov/cgi-bin/GLTRS/browse.pl?2003/TM-2003-212739.html
2. Burke, Kenneth A.: Fuel Cells for Space Science Applications. NASA/TM—2003-212730 (AIAA Paper 2003–5938), 2003. http://gltrs.grc.nasa.gov/cgi-bin/GLTRS/browse.pl?2003/TM-2003-212730.html
3. Ku, Jentung: Operating Characteristics of Loop Heat Pipes. SAE Technical Paper 1999–01–2007, 1999.
4. Baumann, Jane, et al.: A Methodology for Enveloping Reliable Start-up of LHPs. AIAA–2000–2285, 2000.
5. Bauccio, Michael: ASM Metals Reference Book. Third ed., ASM International, Materials Park, OH, 1993.
6. Buch, Alfred: Pure Metals Properties: A Scientific-Technical Handbook. ASM International, Materials Park, OH, 1999.
7. Incropera, Frank P.: Fundamentals of Heat and Mass Transfer. Second ed., John Wiley & Sons, New York, NY, 1985.

8. Zweben, Carl: Composite Materials and Mechanical Design. Mechanical Engineers' Handbook. Second ed., pt. 9, Kutz, Myer, ed., John Wiley & Sons, New York, NY, 1985, pp. 131−190.
9. Holman, J.P.: Heat Transfer. Fourth ed., McGraw-Hill, New York, NY, 1976.
10. Chanda, Manas; and Roy, Salil K.: Plastics Technology Handbook. Third ed., Marcel Dekker, New York, NY, 1998.
11. Missiles and Fire Control. Lockheed Martin. http://www.missilesandfirecontrol.com/our_products/spaceprograms/SPACESTATION/product-spacestation.html Accessed Jan. 26, 2005.
12. Mason, Lee S.: A Power Conversion Concept for the Jupiter Icy Moons Orbiter. AIAA–2003–6007, 2003.

Appendix—Acronyms and Symbols

Acronyms

DOT	Department of Transportation
ISS	International Space Station
LHP	loop heat pipe
PVR	photovoltaic radiator
RFCS	regenerative fuel cell system
URFC	unitized regenerative fuel cell
URFCS	unitized regenerative fuel cell system

Symbols

A	heat radiation area, m^2
A_H	surface area of hydrogen tank, m^2
A_O	surface area of oxygen tank, m^2
$C_{P,H}$	specific heat of the hydrogen tank, kJ/kg/K
$C_{P,HH}$	specific heat of the hydrogen tank, kJ/kg/K
$C_{P,HO}$	specific heat of the oxygen heat pipe, kJ/kg/K
$C_{P,O}$	specific heat of the oxygen tank, kJ/kg/K
dT_{HH}/dt	temperature change rate of H_2 heat pipe, K/h
dT_{HO}/dt	temperature change rate of O_2 heat pipe, K/h
dT_{TH}/dt	temperature change rate of H_2 tank, K/h
dT_{TO}/dt	temperature change rate of O_2 tank, K/h
e	emissivity, dimensionless
e_H	emmisivity of hydrogen tank, dimensionless
e_O	emmisivity of oxygen tank, dimensionless
M_{HH}	mass of the hydrogen heat pipe, kg
M_{HO}	mass of the oxygen heat pipe, kg
M_{TH}	mass of the hydrogen tank, kg
M_{TO}	mass of the oxygen tank, kg
Q	heat radiation rate, W
Q_H	heat radiation from the hydrogen tank, W
Q_O	heat radiation from the oxygen tank, W
σ	5.6703×10^{-8} $W/m^2/K^4$
T	temperature of radiating body, K
T_E	temperature of environment, K
T_{TH}	surface temperature of hydrogen tank, K
T_{TO}	surface temperature of oxygen tank, K

REPORT DOCUMENTATION PAGE

Form Approved
OMB No. 0704-0188

1. AGENCY USE ONLY (*Leave blank*)	2. REPORT DATE	3. REPORT TYPE AND DATES COVERED
	October 2005	Technical Memorandum

4. TITLE AND SUBTITLE

Unitized Regenerative Fuel Cell System Gas Storage-Radiator Development

5. FUNDING NUMBERS

WBS–22–319–20–J1

6. AUTHOR(S)

Kenneth A. Burke and Ian Jakupca

7. PERFORMING ORGANIZATION NAME(S) AND ADDRESS(ES)

National Aeronautics and Space Administration
John H. Glenn Research Center at Lewis Field
Cleveland, Ohio 44135–3191

8. PERFORMING ORGANIZATION REPORT NUMBER

E–14978

9. SPONSORING/MONITORING AGENCY NAME(S) AND ADDRESS(ES)

National Aeronautics and Space Administration
Washington, DC 20546–0001

10. SPONSORING/MONITORING AGENCY REPORT NUMBER

NASA TM—2005-213442

11. SUPPLEMENTARY NOTES

Prepared for the Power Systems Conference sponsored by the Society of Automotive Engineers, Reno, Nevada, November 2–4, 2004. Kenneth A. Burke, NASA Glenn Research Center; and Ian Jakupca, Analex Corporation, Cleveland, Ohio 44135. Responsible person, Kenneth A. Burke, organization code RPC, 216–433–8308.

12a. DISTRIBUTION/AVAILABILITY STATEMENT

Unclassified - Unlimited
Subject Category: 07

Available electronically at http://gltrs.grc.nasa.gov

This publication is available from the NASA Center for AeroSpace Information, 301–621–0390.

12b. DISTRIBUTION CODE

13. ABSTRACT ***(Maximum 200 words)***

High-energy-density regenerative fuel cell systems that are used for energy storage require novel approaches to integrating components in order to preserve mass and volume. A lightweight unitized regenerative fuel cell (URFC) energy storage system concept is being developed at the NASA Glenn Research Center. This URFC system minimizes mass by using the surface area of the hydrogen and oxygen storage tanks as radiating heat surfaces for overall thermal control of the system. The waste heat generated by the URFC stack during charging and discharging is transferred from the cell stack to the surface of each tank by loop heat pipes, which are coiled around each tank and covered with a thin layer of thermally conductive carbon composite. The thin layer of carbon composite acts as a fin structure that spreads the heat away from the heat pipe and across the entire tank surface. Two different-sized commercial-grade composite tanks were constructed with integral heat pipes and tested in a thermal vacuum chamber to examine the feasibility of using the storage tanks as system radiators. The storage tank-radiators were subjected to different steady-state heat loads and varying heat load profiles. The surface emissivity and specific heat capacity of each tank were calculated. In the future, the results will be incorporated into a model that simulates the performance of similar radiators using lightweight, space-rated carbon composite tanks.

14. SUBJECT TERMS

Temperature control; Energy storage; Heat pipes; Storage tanks; Regenerative fuel cells; Radiators

15. NUMBER OF PAGES

25

16. PRICE CODE

17. SECURITY CLASSIFICATION OF REPORT	18. SECURITY CLASSIFICATION OF THIS PAGE	19. SECURITY CLASSIFICATION OF ABSTRACT	20. LIMITATION OF ABSTRACT
Unclassified	Unclassified	Unclassified	